Near-Degenerate Quadrature-Squeezed Vacuum Generation on a Silicon-Nitride Chip

Yun Zhao,[1,*] Yoshitomo Okawachi,[2] Jae K. Jang,[2] Xingchen Ji,[1] Michal Lipson,[1,2] and Alexander L. Gaeta[1,2]
[1]Department of Electrical Engineering, Columbia University, New York, New York 10027, USA
[2]Department of Applied Physics and Applied Mathematics, Columbia University, New York, New York 10027, USA

(Received 3 February 2020; accepted 21 April 2020; published 12 May 2020)

Squeezed states are a primary resource for continuous-variable (CV) quantum information processing. To implement CV protocols in a scalable and robust way, it is desirable to generate and manipulate squeezed states using an integrated photonics platform. In this Letter, we demonstrate the generation of quadrature-phase squeezed states in the radio-frequency carrier sideband using a small-footprint silicon-nitride microresonator with a dual-pumped four-wave-mixing process. We record a squeezed noise level of 1.34 dB (±0.16 dB) below the photocurrent shot noise, which corresponds to 3.09 dB (±0.49 dB) of quadrature squeezing on chip. We also show that it is critical to account for the nonlinear behavior of the pump fields to properly predict the squeezing that can be generated in this system. This technology represents a significant step toward creating and manipulating large-scale CV cluster states that can be used for quantum information applications, including universal quantum computing.

DOI: 10.1103/PhysRevLett.124.193601

Quantum optics can revolutionize information acquisition and processing, including sensing [1,2], communication [3], and computation [4], by offering new paradigms to achieve performance that is superior to classical approaches. The implementation of such schemes requires the use of nonclassical states of light, where information can be carried by both discrete (DV) and continuous (CV) quantum variables. The quantum sources required to implement most DV and CV protocols are single photons and squeezed light, respectively. Compared to the DV information processing, CV schemes provide powerful alternatives with unique features, such as high efficiency state characterization and unconditional state manipulation [5]. Recently, the demand of scalability in quantum information processing has stimulated efforts to produce quantum light sources on a photonic chip. While fully integrated quasideterministic single photons have been used in proof-of-principle quantum information protocols [6], the on-chip generation of squeezed light that is suitable for CV protocols remains challenging and has shown less scalability due to the large feature sizes and long fabrication times in reported experiments [7–12].

Squeezed states represent a key resource for CV quantum information processing, with applications in universal quantum computing [13,14], quantum error correction [15,16], quantum teleportation [17], quantum secret sharing [18], and quantum key distribution [19]. There are many ways to generate a quadrature-squeezed state optically, most of which are based on the three pioneering experiments reported during 1985 and 1986, namely, noncollinear degenerate four-wave mixing in atomic ensembles [20], self-phase modulation (SPM) in a $\chi^{(3)}$ medium [21], and degenerate parametric down-conversion (DPDC) in a $\chi^{(2)}$ medium [22]. It is worth noting that the nonlinear processes are degenerate for the carrier frequency, while noise squeezing arises from photon correlations at nearby frequency sidebands, which are nondegenerate. To date, most of the chip-based squeezed state generations rely on the DPDC process [7–11], however, the large-scale integration of and fabrication on $\chi^{(2)}$ materials remains challenging.

As an alternative, researchers have investigated the generation of squeezed states on a platform compatible with the standard complementary metal oxide semiconductor (CMOS) process on a silicon chip, which provides a scalable solution for CV quantum sources. This calls for a squeezing process with $\chi^{(3)}$ nonlinearity in a small-footprint structure. The first direct observation of photocurrent noise squeezing on a silicon chip was shown by Dutt *et al.* in a silicon-nitride (SiN) microresonator [23], in which a spontaneous four-wave-mixing (SFWM) process was employed and a reduction was observed in the relative intensity fluctuations between bright signal and idler beams below the shot-noise level. Recently, Vaidya *et al.* [24] successfully observed quadrature-phase squeezing with the SFWM scheme operating below oscillation threshold. However, the squeezed sidebands are generated from two largely separated (190 GHz) cavity modes and can only be measured via a bichromatic heterodyne measurement [25]. Many current CV protocols require single-spatiotemporal-mode squeezed states [26], which is incompatible with this two-mode squeezing scheme. An alternative on-chip squeezing scheme is demonstrated by Cernansky and Politi, which uses SPM [27]. Quadrature squeezing was observed for frequencies above 500 MHz.

However, a large amount of excess noise was observed for lower frequencies due to their close proximity to the strong pump.

In this Letter, we generate quadrature squeezing near the degenerate carrier frequency by employing a dual-pumped degenerate four-wave-mixing (DPFWM) scheme [28], in which two pump fields provide parametric gain for the degenerate signal field at a frequency centered between those of the pump fields [Fig. 1(b)]. This scheme can be viewed as the $\chi^{(3)}$ counterpart to the DPDC process [Fig. 1(a)], where the upper virtual transition level is driven by two pump fields rather than by one. Previously, this DPFWM scheme has been used for on-chip random number generation [29], degenerate photon-pair generation [30], and boson sampling [31]. The possibility of using it to generate squeezed states was recently studied theoretically by Vernon *et al.* [26], but no experimental demonstration has been shown prior to this Letter.

Our on-chip squeezing device is based on the SiN-on-insulator platform, which has the advantage of extremely low propagation loss and large-scale monolithically integrability. It has been widely used in photonics research with both classical and quantum applications [34–36]. Particularly, its low propagation loss (≈0.28 dB/ cm for the current device and 0.08 dB/cm has been shown [37]) and ease of fabrication allow for implementation of cavity-enhanced squeezing schemes on chip, which greatly boosts the squeezing level and shrinks the device footprint. Quadrature-squeezed states are best characterized by homodyne measurements that are also essential to CV quantum information protocols. To perform a homodyne measurement, a local oscillator (LO) that is phase coherent with the squeezed state is required. In this Letter, we generate the squeezed state and a coherent LO on the same chip simultaneously. We fabricate two identical ring resonators that are evanescently coupled to their respective bus waveguides with the coupling gaps chosen such that one ring is critically coupled (i.e., round-trip coupling ratio = round-trip propagation loss ratio) and the other is overcoupled (i.e., round-trip coupling ratio > round-trip propagation loss ratio). Consequently, the overcoupled ring has a higher oscillation threshold. For the current experiment, the overcoupled ring has an escape efficiency of 2/3 (i.e., loaded Q is 3× that of the intrinsic Q) and the intrinsic Q of the microresonators is measured to be 1.3×10^6. Each SiN ring has a platinum microheater above the silicon dioxide cladding to adjust for any mismatch in resonance frequencies that arises from accumulated phase shifts in the coupling region and nonuniform material strains across the chip. Platinum is chosen for its CMOS-process compatibility, inert chemical properties, and high heat tolerance. The two bus waveguides split the pumps evenly through a multimode interferometric beam splitter at the input. When the pump frequencies are tuned to the resonant modes of both microresonators, the critically coupled ring oscillates, producing a bright local oscillator, and the overcoupled ring remains below threshold, generating a squeezed state. The matching of the transverse-mode profiles between the LO and the squeezed state are naturally achieved by this scheme since they are generated in the same waveguide mode. Henceforth, we will refer to the critically coupled ring as the oscillator and the overcoupled ring as the squeezer.

Two stable states with a π phase difference are supported by the oscillator [38,39]. Each time the pump fields are turned on, the LO settles into one of two stable phases. However, for the purpose of this experiment, the two states yield the same results since a π phase shift of the LO results in a measurement on the same quadrature component. To ensure that degenerate oscillation is the dominant nonlinear process, we dispersion engineer the microresonators to have small normal group-velocity dispersion (GVD) at the degenerate frequency such that the parametric gain peaks at this frequency. More information concerning the design and dispersion engineering of this degenerate oscillator can be found in [28]. The experimental characterization of the LO is shown in the Supplemental Material [32], which includes Refs. [37,40–42].

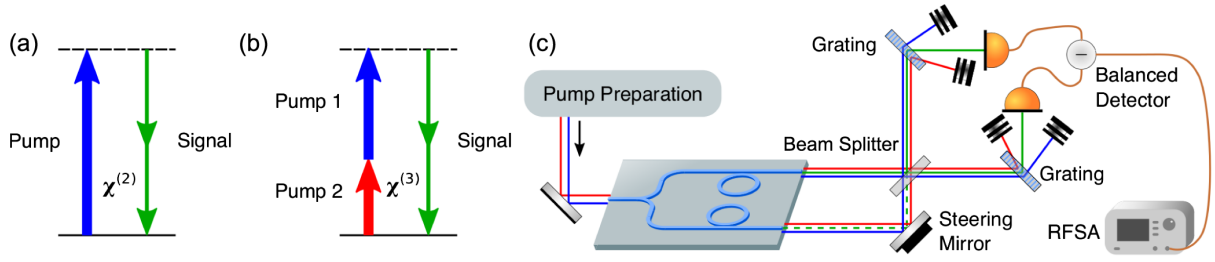

FIG. 1. (a) The DPDC process used in $\chi^{(2)}$-based squeezing, and (b) the DPFWM process used in this experiment for on-silicon-chip squeezing. (c) Experimental schematic (not to scale). Two pump lasers at 1543 and 1559 nm are coupled onto the chip, which simultaneously generates a squeezed state and a LO. The two output fields are overlapped on a 50/50 beam splitter with the arm length difference controlled by a piezo steering mirror. After the beam splitter, the pump fields are separated from the signal fields with two transmission gratings. The signal fields are then detected by a balanced photodetector, and the rf signal is recorded by a rf spectrum analyzer (RFSA). The full experiment schematic including pump preparation and stabilization is presented in the Supplemental Material [32], which includes Ref. [33].

A critical aspect for this dual-pumped system is that it can display rich nonlinear dynamics due to the existence of SPM and cross-phase modulation (XPM) [43]. To more fully understand the dynamics of each resonator, we model the pump and signal evolution with the same set of three-coupled-mode equations [44],

$$\frac{dA_b}{dt} = i\gamma L f_\delta(|A_b|^2 + 2|A_r|^2 + 2|A_s|^2)A_b + i\gamma L f_\delta A_r^* A_s^2 - \left(\frac{\alpha+\theta}{2} + i\delta_b\right)A_b + \sqrt{\theta f_\delta P_b}, \quad (1)$$

$$\frac{dA_r}{dt} = i\gamma L f_\delta(2|A_b|^2 + |A_r|^2 + 2|A_s|^2)A_r + i\gamma L f_\delta A_b^* A_s^2 - \left(\frac{\alpha+\theta}{2} + i\delta_r\right)A_r + \sqrt{\theta f_\delta P_r}, \quad (2)$$

$$\frac{dA_s}{dt} = i\gamma L f_\delta(2|A_r|^2 + 2|A_b|^2 + |A_s|^2)A_s + i2\gamma L f_\delta A_s^* A_b A_r - \left(\frac{\alpha+\theta}{2} + i\delta_\beta\right)A_s, \quad (3)$$

where A_i $(i = b, r, s)$ are the amplitudes of the short-wavelength (blue) pump, long-wavelength (red) pump, and the signal fields, respectively, α is the scattering loss rate, θ is the bus-ring coupling rate, f_δ is the free spectral range (FSR), γ is the nonlinear coefficient, L is the cavity length, P_i $(i = b, r)$ are the input pump powers, and δ_i $(i = b, r)$ are the pump detunings with respect to the linear cavity resonances in angular frequencies. We choose the convention such that $\delta_i > 0$ indicates red detuning. $\delta_\beta = \delta_b/2 + \delta_r/2 + 2\pi^2\beta_2 L m^2 f_\delta^3$ is the signal detuning due to second-order dispersion, where β_2 is the GVD coefficient and m is the mode index difference between the pump and the signal. We normalize the field amplitudes such that $|A_i|^2$ represents the average power in the cavity. The α and θ parameters can be directly related to the intrinsic and loaded Q factors Q_i and Q_l as $\alpha = \omega/Q_i$ and $\alpha + \theta = \omega/Q_l$, where ω is the angular frequency of the signal field. The complex nonlinear dynamics can be illustrated by plotting the bifurcation behaviors of the system. We fix the detuning of the red pump and sweep the detuning of the blue pump while searching for all equilibrium states (Fig. 2). The stable states are shown in solid lines and the unstable states are shown in dashed lines. In the oscillator ring, a signal field is generated with a small-detuned blue pump if the red pump is initially on the lower branch of the equilibrium states (darker lines). We show examples of other equilibrium states that are supported within the same detuning parameter space with lighter lines, which need to be avoided as they are unsuitable for either LO or squeezed state generation. The squeezer ring is identical to the oscillator ring, except for a higher bus-ring coupling rate (θ). Importantly, as their

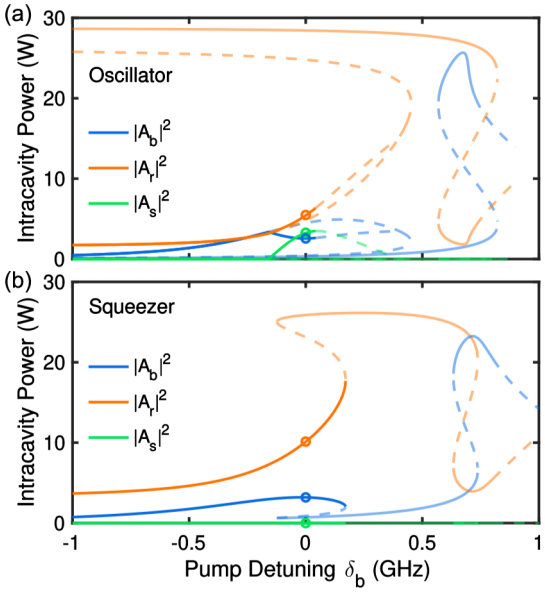

FIG. 2. Numerical simulation of equilibrium states in a dual-pumped $\chi^{(3)}$ cavity. For clarity, some equilibrium states are not shown. Stable states are plotted in solid lines and unstable states in dashed lines. Dark lines indicate the branch accessed in the experiment and light lines indicate the branches to avoid. The states corresponding to the final experimental condition are shown in circles. The simulation parameters are chosen as $\delta_r = 2\pi \times 650$ MHz, $\gamma = 1$ W^{-1} m^{-1}, $L = 230$ μm, $f_\delta = 2\pi \times 500$ GHz, $P_b = 48$ mW, $P_r = 54$ mW, $\alpha = 2\pi \times 150$ MHz, (a) $\theta = 2\pi \times 150$ MHz, and (b) $\theta = 2\pi \times 300$ MHz.

pumps are derived from the same laser sources, both the oscillator and the squeezer operate under the same detuning conditions. To generate a squeezed state, it is necessary to operate below oscillation threshold while keeping a high intracavity power of both pumps. By examining Fig. 2(b), we find that it can be achieved by the same branch of equilibrium states as the oscillation branch in Fig. 2(a). Experimentally, this branch of states can be accessed by tuning the red pump from a long wavelength to the desired detuning value (650 MHz red detuned) followed by tuning the blue pump from a short wavelength into the resonance. The experiment is performed at the detunings that have a LO power slightly lower than the maximum power (Supplemental Material [32]). The corresponding equilibrium states are indicated by circles in Fig. 2. Under nearly all conditions, the intracavity powers of the two pump fields are not equal even for equal input powers due to their tendency to repel each other at high powers [43]. This can make both the optical parametric oscillation and the squeezing processes less energy efficient, but poses no fundamental limit to the attainable squeezing level.

The output spectrum of the LO ring is shown in Fig. 3(a). The two pump fields are at 1543 and 1559 nm, respectively, and the LO is generated at 1551 nm, two FSRs away from the pump resonances. We also observe frequency components generated by other four-wave-mixing (FWM)

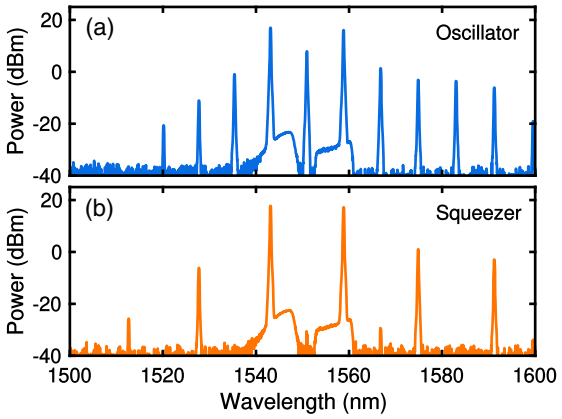

FIG. 3. Output spectra from the oscillator (a) and the squeezer (b), respectively. The FSR of the devices is 4 nm (500 GHz).

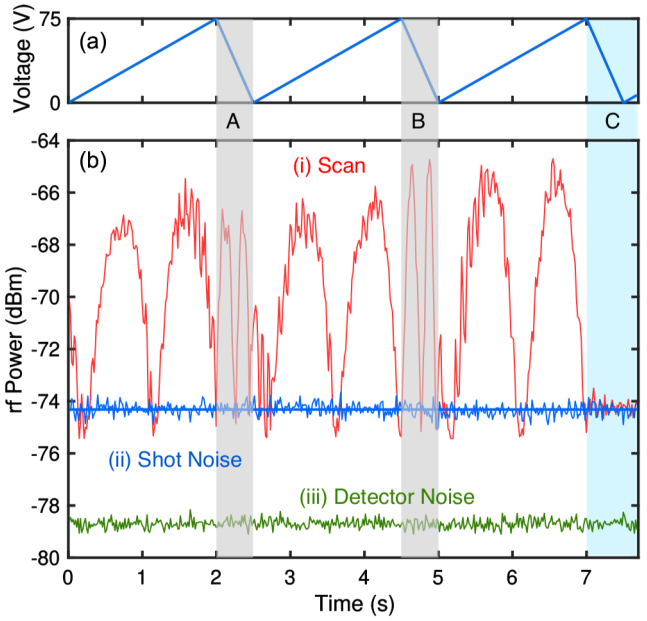

FIG. 4. (a) Piezoscan voltage and (b) detected rf noise power while the delay is scanned, (i) with the squeezed state, (ii) without the squeezed state, and (iii) without light. Shaded regions *A* and *B* correspond to the return part of the scan. After the third scan, we block the squeezed state to record an extra copy of the shot noise, which is shown in shaded region *C*.

processes, but they are sufficiently weak and far detuned from the LO that they can be neglected. The LO light is easily separated from the other frequency components with a grating [Fig. 1(c)] owing to the large FSR of microcavities. The spectrum corresponding to squeezed state generation is shown in Fig. 3(b). The small peak at the signal wavelength (1551 nm) is due to the backreflection from the facets of waveguides (≈4% per facet) and the backscattering of the LO microresonator. This spurious signal is measured to be more than 40 dB lower than that of the LO. The effect of a weak seed laser on squeezing has been studied in the context of coherent control of squeezed states and has been found to be tolerable for low power seeds or high frequency detection sidebands [45,46]. It is also possible to further eliminate this spurious signal by using angled waveguide facets or a filter ring before the squeezer. The other bright frequency components in Fig. 3(b) are a result of stimulated FWM processes, whose effects are negligible for squeezed state generation near the degenerate point.

To characterize the squeezed state with a homodyne measurement [Fig. 1(c)], we interfere the two output beams (including all frequency components) from the chip on a beam splitter (Thorlabs CCM5-BS018, $T = 42\%$, $R = 47\%$). We use two transmission gratings (LightSmyth T-966C-1610-90) to spatially separate the different frequency modes of the output, for which 97% of the light goes into the first diffraction order. In principle, the beam splitter can be replaced by an on-chip evanescent coupler, and the gratings can be replaced by on-chip add-drop ring filters, both of which have negligible losses. The two LO beams after the gratings are collected into high numerical aperture fibers (Thorlabs FP200ERT) and detected by fiber-coupled balanced detectors (Thorlabs PDB150C). We use a polarizer (Thorlabs LPNIR050) to balance the dc photocurrents of the two photodiodes (PDs), where the initial imbalance arises from the imperfect splitting ratio of the beam splitter and the unequal responsivities of the PDs. We use a piezosteering mirror on the squeezer path to control the relative delay between the squeezed state and the LO. A maximum scanning voltage of 75 V corresponds to a phase change of $\approx 2.6\pi$. Figure 4 shows the photocurrent noise for three scanning periods at a sideband frequency of 40 MHz, with a resolution bandwidth of 100 kHz and a video bandwidth of 100 Hz. At the end of the third scan, we block the squeezed state and record the shot-noise level. For a clear comparison, we record a second copy of the shot noise for a same time span as the scan with the squeezed state blocked, which shows excellent agreement with the first shot-noise measurement, which indicates that the generated LO is stable. In Fig. 4(b), the scanned signal dips below the shot-noise level, which indicates squeezing. The high fluctuation level of the antisqueezed quadrature indicates that the squeezer is operated close to oscillation threshold. From Fig. 4(b), we obtain a directly observed squeezing level of 0.81 ± 0.09 dB, where the uncertainty is taken as the standard error of the measurement (Supplemental Material [32]). The low detector dark-noise clearance also artificially reduces the measured squeezing level. This effect can be removed by a simple numerical subtraction, which yields a detector noise corrected squeezing level of 1.34 ± 0.16 dB. The measured squeezing level is also reduced by the losses in the measurement system. We estimate the total loss to be 48%, including Fresnel reflection losses, mirror losses, beam splitter loss, grating losses, and the detector quantum efficiency. After correcting for these losses, we infer an on-chip squeezing level of 3.09 ± 0.49 dB.

Similar to squeezing in a $\chi^{(2)}$ cavity, the level of squeezing from our $\chi^{(3)}$ microresonator is ultimately limited by the cavity scattering losses and the output coupling ratio. However, due to the proximity between the pump fields and the signal in our scheme, other parasitic $\chi^{(3)}$ processes can occur. The nonlinear processes of SPM and XPM modify the cavity detuning of the squeezed signal, but do not change the maximum squeezing level that is achieved near oscillation threshold. The more deleterious processes are SFWM and FWM Bragg scattering processes [26] that couple the squeezed mode to other cavity modes, which degrades the tight field correlation between the upper and lower frequency sidebands of the squeezed mode. Indeed, a theoretical model including all parasitic processes (see Supplemental Material [32], which includes Refs. [26,47–50]) shows that no more than 0.8 dB of squeezing can be generated if these processes are unmitigated. The operation regime (circles in Fig. 2) in this experiment is chosen to suppress the parasitic processes based on their different phase-matching conditions compared to the DPFWM process. We present a detailed analysis in the Supplemental Material [32], where we show that the pump state in Fig. 2(b) leads to a theoretical squeezing level of 3.5 dB, agreeing with the experimental observation.

In conclusion, we experimentally demonstrate the first silicon-chip-based generation of quadrature-phase squeezed states in the rf carrier sideband. This also represents the first time photocurrent noise squeezing is observed from the DPFWM process. We also show that the pump waves can exhibit rich nonlinear dynamical behavior that determines the squeezing levels. The SiN platform we used for squeezing is a mature technology for large-scale fabrication of linear optical components which, combined with squeezed states, can be used to form entangled CV states [51] and CV cluster states. More details about combining the on-chip squeezed states with currently available integrated beam splitters and detectors for quantum information processing can be found in the Supplemental Material [32], which includes Refs. [52–64]. We believe this technology represents a significant step toward the fully on-chip implementation of CV quantum protocols and possibly photonic-based universal quantum computers.

We thank Professor Imad Agha, Dr. Chaitanya Joshi, Dr. Avik Dutt, Chaitali Joshi, and Bok Young Kim for helpful discussions. This work was supported by Army Research Office (ARO) (Grant No. W911NF-17-1-0016), National Science Foundation (NSF) (Grants No. CCF-1640108, EFMA-1641094), Semiconductor Research Corporation (SRC) (Grant No. SRS 2016-EP-2693-A), and Air Force Office of Scientific Research (AFOSR) (Grant No. FA9550-15-1-0303). This work was performed in part at the Cornell Nano-Scale Facility, which is a member of the National Nanotechnology Infrastructure Network, supported by the NSF, and at the CUNY Advanced Science Research Center NanoFabrication Facility.

Note added.—Recently, another study on squeezed state generation based on the SiN platform was reported [65].

*yz3019@columbia.edu

[1] C. M. Caves, Quantum-mechanical noise in an interferometer, Phys. Rev. D **23**, 1693 (1981).
[2] V. Giovannetti, S. Lloyd, and L. Maccone, Advances in quantum metrology, Nat. Photonics **5**, 222 (2011).
[3] V. Scarani, H. Bechmann-Pasquinucci, N. J. Cerf, M. Dušek, N. Lütkenhaus, and M. Peev, The security of practical quantum key distribution, Rev. Mod. Phys. **81**, 1301 (2009).
[4] P. Kok, W. J. Munro, K. Nemoto, T. C. Ralph, J. P. Dowling, and G. J. Milburn, Linear optical quantum computing with photonic qubits, Rev. Mod. Phys. **79**, 135 (2007).
[5] S. L. Braunstein and P. van Loock, Quantum information with continuous variables, Rev. Mod. Phys. **77**, 513 (2005).
[6] X. Qiang, X. Zhou, J. Wang, C. M. Wilkes, T. Loke, S. OGara, L. Kling, G. D. Marshall, R. Santagati, T. C. Ralph, J. B. Wang, J. L. OBrien, M. G. Thompson, and J. C. F. Matthews, Large-scale silicon quantum photonics implementing arbitrary two-qubit processing, Nat. Photonics **12**, 534 (2018).
[7] M. E. Anderson, M. Beck, M. G. Raymer, and J. D. Bierlein, Quadrature squeezing with ultrashort pulses in nonlinear-optical waveguides, Opt. Lett. **20**, 620 (1995).
[8] D. K. Serkland, M. M. Fejer, R. L. Byer, and Y. Yamamoto, Squeezing in a quasi-phase-matched $LiNbO_3$ waveguide, Opt. Lett. **20**, 1649 (1995).
[9] G. S. Kanter, P. Kumar, R. V. Roussev, J. Kurz, K. R. Parameswaran, and M. M. Fejer, Squeezing in a $LiNbO_3$ integrated optical waveguide circuit, Opt. Express **10**, 177 (2002).
[10] F. Mondain, T. Lunghi, A. Zavatta, E. Gouzien, F. Doutre, M. D. Micheli, S. Tanzilli, and V. D'Auria, Chip-based squeezing at a telecom wavelength, Photonics Res. **7**, A36 (2019).
[11] F. Lenzini, J. Janousek, O. Thearle, M. Villa, B. Haylock, S. Kasture, L. Cui, H.-P. Phan, D. V. Dao, H. Yonezawa, P. K. Lam, E. H. Huntington, and M. Lobino, Integrated photonic platform for quantum information with continuous variables, Sci. Adv. **4**, eaat9331 (2018).
[12] A. Otterpohl, F. Sedlmeir, U. Vogl, T. Dirmeier, G. Shafiee, G. Schunk, D. V. Strekalov, H. G. L. Schwefel, T. Gehring, U. L. Andersen, G. Leuchs, and C. Marquardt, Squeezed vacuum states from a whispering gallery mode resonator, Optica **6**, 1375 (2019).
[13] S. Lloyd and S. L. Braunstein, Quantum Computation over Continuous Variables, Phys. Rev. Lett. **82**, 1784 (1999).
[14] N. C. Menicucci, P. van Loock, M. Gu, C. Weedbrook, T. C. Ralph, and M. A. Nielsen, Universal Quantum Computation with Continuous-Variable Cluster States, Phys. Rev. Lett. **97**, 110501 (2006).

[15] S. L. Braunstein, Error Correction for Continuous Quantum Variables, Phys. Rev. Lett. **80**, 4084 (1998).
[16] S. Lloyd and Jean-Jacques E. Slotine, Analog Quantum Error Correction, Phys. Rev. Lett. **80**, 4088 (1998).
[17] S. L. Braunstein and H. J. Kimble, Teleportation of Continuous Quantum Variables, Phys. Rev. Lett. **80**, 869 (1998).
[18] H.-K. Lau and C. Weedbrook, Quantum secret sharing with continuous-variable cluster states, Phys. Rev. A **88**, 042313 (2013).
[19] D. Gottesman and J. Preskill, Secure quantum key distribution using squeezed states, Phys. Rev. A **63**, 022309 (2001).
[20] R. E. Slusher, L. W. Hollberg, B. Yurke, J. C. Mertz, and J. F. Valley, Observation of Squeezed States Generated by Four-Wave Mixing in an Optical Cavity, Phys. Rev. Lett. **55**, 2409 (1985).
[21] R. M. Shelby, M. D. Levenson, S. H. Perlmutter, R. G. DeVoe, and D. F. Walls, Broad-Band Parametric Deamplification of Quantum Noise in an Optical Fiber, Phys. Rev. Lett. **57**, 691 (1986).
[22] L.-A. Wu, H. J. Kimble, J. L. Hall, and H. Wu, Generation of Squeezed States by Parametric Down Conversion, Phys. Rev. Lett. **57**, 2520 (1986).
[23] A. Dutt, K. Luke, S. Manipatruni, A. L. Gaeta, P. Nussenzveig, and M. Lipson, On-Chip Optical Squeezing, Phys. Rev. Applied **3**, 044005 (2015).
[24] V. D. Vaidya, B. Morrison, L. G. Helt, R. Shahrokhshahi, D. H. Mahler, M. J. Collins, K. Tan, J. Lavoie, A. Repingon, M. Menotti, N. Quesada, R. C. Pooser, A. E. Lita, T. Gerrits, S. W. Nam, and Z. Vernon, Broadband quadrature-squeezed vacuum and nonclassical photon number correlations from a nanophotonic device, arXiv:1904.07833.
[25] A. M. Marino, J. C. R. Stroud, V. Wong, R. S. Bennink, and R. W. Boyd, Bichromatic local oscillator for detection of two-mode squeezed states of light, J. Opt. Soc. Am. B **24**, 335 (2007).
[26] Z. Vernon, N. Quesada, M. Liscidini, B. Morrison, M. Menotti, K. Tan, and J. E. Sipe, Scalable Squeezed-Light Source for Continuous-Variable Quantum Sampling, Phys. Rev. Applied **12**, 064024 (2019).
[27] R. Cernansky and A. Politi, Nanophotonic source of broadband quadrature squeezing, arXiv:1904.07283.
[28] Y. Okawachi, M. Yu, K. Luke, D. O. Carvalho, S. Ramelow, A. Farsi, M. Lipson, and A. L. Gaeta, Dual-pumped degenerate Kerr oscillator in a silicon nitride microresonator, Opt. Lett. **40**, 5267 (2015).
[29] Y. Okawachi, M. Yu, K. Luke, D. O. Carvalho, M. Lipson, and A. L. Gaeta, Quantum random number generator using a microresonator-based Kerr oscillator, Opt. Lett. **41**, 4194 (2016).
[30] J. He, B. A. Bell, A. Casas-Bedoya, Y. Zhang, A. S. Clark, C. Xiong, and B. J. Eggleton, Ultracompact quantum splitter of degenerate photon pairs, Optica **2**, 779 (2015).
[31] S. Paesani, Y. Ding, R. Santagati, L. Chakhmakhchyan, C. Vigliar, K. Rottwitt, L. K. Oxenlwe, J. Wang, M. G. Thompson, and A. Laing, Generation and sampling of quantum states of light in a silicon chip, Nat. Phys. **15**, 925 (2019).
[32] See Supplemental Material at http://link.aps.org/supplemental/10.1103/PhysRevLett.124.193601 for (i) more information about the experiment scheme, measurements, and data analysis, which includes Refs. [37,40–42], (ii) a theoretical model describing the squeezed state generation with the effect of parasitic nonlinear processes, which includes Refs. [26,47–50], and (iii) a brief discussion about the path toward chip-based large-scale CV quantum information processing, which includes Refs. [52–64].
[33] T. Carmon, L. Yang, and K. J. Vahala, Dynamical thermal behavior and thermal self-stability of microcavities, Opt. Express **12**, 4742 (2004).
[34] D. J. Moss, R. Morandotti, A. L. Gaeta, and M. Lipson, New CMOS-compatible platforms based on silicon nitride and Hydex for nonlinear optics, Nat. Photonics **7**, 597 (2013).
[35] A. L. Gaeta, M. Lipson, and T. J. Kippenberg, Photonic-chip-based frequency combs, Nat. Photonics **13**, 158 (2019).
[36] M. Kues, C. Reimer, J. M. Lukens, W. J. Munro, A. M. Weiner, D. J. Moss, and R. Morandotti, Quantum optical microcombs, Nat. Photonics **13**, 170 (2019).
[37] X. Ji, F. A. S. Barbosa, S. P. Roberts, A. Dutt, J. Cardenas, Y. Okawachi, A. Bryant, A. L. Gaeta, and M. Lipson, Ultra-low-loss on-chip resonators with sub-milliwatt parametric oscillation threshold, Optica **4**, 619 (2017).
[38] R. Graham and F. Haake, *Quantum Statistics in Optics and Solid-State Physics*, Springer Tracts in Modern Physics, Vol. 66 (Springer, Berlin, 1973).
[39] P. D. Drummond and P. Kinsler, Quantum tunneling and thermal activation in the parametric oscillator, Phys. Rev. A **40**, 4813 (1989).
[40] T. Okoshi, K. Kikuchi, and A. Nakayama, Novel method for high resolution measurement of laser output spectrum, Electron. Lett. **16**, 630 (1980).
[41] N. Le Thomas, A. Dhakal, A. Raza, F. Peyskens, and R. Baets, Impact of fundamental thermodynamic fluctuations on light propagating in photonic waveguides made of amorphous materials, Optica **5**, 328 (2018).
[42] G. Huang, E. Lucas, J. Liu, A. S. Raja, G. Lihachev, M. L. Gorodetsky, N. J. Engelsen, and T. J. Kippenberg, Thermorefractive noise in silicon-nitride microresonators, Phys. Rev. A **99**, 061801(R) (2019).
[43] L. Del Bino, J. M. Silver, S. L. Stebbings, and P. Del'Haye, Symmetry breaking of counter-propagating light in a nonlinear resonator, Sci. Rep. **7**, 43142 (2017).
[44] Y. K. Chembo and N. Yu, Modal expansion approach to optical-frequency-comb generation with monolithic whispering-gallery-mode resonators, Phys. Rev. A **82**, 033801 (2010).
[45] K. McKenzie, N. Grosse, W. P. Bowen, S. E. Whitcomb, M. B. Gray, D. E. McClelland, and P. K. Lam, Squeezing in the Audio Gravitational-Wave Detection Band, Phys. Rev. Lett. **93**, 161105 (2004).
[46] K. Goda, K. McKenzie, E. E. Mikhailov, P. K. Lam, D. E. McClelland, and N. Mavalvala, Photothermal fluctuations as a fundamental limit to low-frequency squeezing in a degenerate optical parametric oscillator, Phys. Rev. A **72**, 043819 (2005).
[47] M. J. Collett and C. W. Gardiner, Squeezing of intracavity and traveling-wave light fields produced in parametric amplification, Phys. Rev. A **30**, 1386 (1984).

[48] Z. Vernon and J. E. Sipe, Spontaneous four-wave mixing in lossy microring resonators, Phys. Rev. A **91**, 053802 (2015).

[49] Y. Zhao, X. Ji, B. Y. Kim, P. S. Donvalkar, J. K. Jang, C. Joshi, M. Yu, C. Joshi, R. R. Domeneguetti, F. A. S. Barbosa, P. Nussenzveig, Y. Okawachi, M. Lipson, and A. L. Gaeta, Visible nonlinear photonics via high-order-mode dispersion engineering, Optica **7**, 135 (2020).

[50] B. E. Little, S. T. Chu, H. A. Haus, J. Foresi, and J. P. Laine, Microring resonator channel dropping filters, J. Lightwave Technol. **15**, 998 (1997).

[51] G. Masada, K. Miyata, A. Politi, T. Hashimoto, J. L. O'Brien, and A. Furusawa, Continuous-variable entanglement on a chip, Nat. Photonics **9**, 316 (2015).

[52] J. Huh, G. G. Guerreschi, B. Peropadre, J. R. McClean, and A. Aspuru-Guzik, Boson sampling for molecular vibronic spectra, Nat. Photonics **9**, 615 (2015).

[53] N. C. Menicucci, Fault-Tolerant Measurement-Based Quantum Computing with Continuous-Variable Cluster States, Phys. Rev. Lett. **112**, 120504 (2014).

[54] K. Fukui, A. Tomita, A. Okamoto, and K. Fujii, High-Threshold Fault-Tolerant Quantum Computation with Analog Quantum Error Correction, Phys. Rev. X **8**, 021054 (2018).

[55] J. Carolan, C. Harrold, C. Sparrow, E. Martín-López, N. J. Russell, J. W. Silverstone, P. J. Shadbolt, N. Matsuda, M. Oguma, M. Itoh, G. D. Marshall, M. G. Thompson, J. C. F. Matthews, T. Hashimoto, J. L. O'Brien, and A. Laing, Universal linear optics, Science **349**, 711 (2015).

[56] B. Calkins, P. L. Mennea, A. E. Lita, B. J. Metcalf, W. S. Kolthammer, A. Lamas-Linares, J. B. Spring, P. C. Humphreys, R. P. Mirin, J. C. Gates, P. G. R. Smith, I. A. Walmsley, T. Gerrits, and S. W. Nam, High quantum-efficiency photon-number-resolving detector for photonic on-chip information processing, Opt. Express **21**, 22657 (2013).

[57] F. Raffaelli, G. Ferranti, D. H. Mahler, P. Sibson, J. E. Kennard, A. Santamato, G. Sinclair, D. Bonneau, M. G. Thompson, and J. C. F. Matthews, A homodyne detector integrated onto a photonic chip for measuring quantum states and generating random numbers, Quantum Sci. Technol. **3**, 025003 (2018).

[58] C. Porto, D. Rusca, S. Cialdi, A. Crespi, R. Osellame, D. Tamascelli, S. Olivares, and M. G. A. Paris, Detection of squeezed light with glass-integrated technology embedded into a homodyne detector setup, J. Opt. Soc. Am. B **35**, 1596 (2018).

[59] Q. Yu, K. Sun, Q. Li, and A. Beling, Segmented waveguide photodetector with 90% quantum efficiency, Opt. Express **26**, 12499 (2018).

[60] J. Piprek, D. Lasaosa, D. Pasquariello, and J. E. Bowers, Physics of waveguide photodetectors with integrated amplification, in *Physics and Simulation of Optoelectronic Devices XI* edited by M. Osinski, H. Amano, and P. Blood (SPIE, San Jose, CA, 2003), Vol. 4986, pp. 214–221, https://doi.org/10.1117/12.473078.

[61] Y. Lin, K. H. Lee, S. Bao, X. Guo, H. Wang, J. Michel, and C. S. Tan, High-efficiency normal-incidence vertical p-i-n photodetectors on a germanium-on-insulator platform, Photonics Res. **5**, 702 (2017).

[62] H. Vahlbruch, M. Mehmet, K. Danzmann, and R. Schnabel, Detection of 15 dB Squeezed States of Light and Their Application for the Absolute Calibration of Photoelectric Quantum Efficiency, Phys. Rev. Lett. **117**, 110801 (2016).

[63] D. Oser, S. Tanzilli, F. Mazeas, C. Alonso-Ramos, X. L. Roux, G. Sauder, X. Hua, O. Alibart, L. Vivien, E. Cassan, and L. Labonté, High-quality photonic entanglement based on a silicon chip, arXiv:2002.10106.

[64] B. Q. Baragiola, G. Pantaleoni, R. N. Alexander, A. Karanjai, and N. C. Menicucci, All-Gaussian Universality and Fault Tolerance with the Gottesman-Kitaev-Preskill Code, Phys. Rev. Lett. **123**, 200502 (2019).

[65] Y. Zhang, M. Menotti, K. Tan, V. D. Vaidya, D. H. Mahler, L. Zatti, M. Liscidini, B. Morrison, and Z. Vernon, Single-mode quadrature squeezing using dual-pump four-wave mixing in an integrated nanophotonic device, arXiv:2001.09474.